Delineating the DNA damage response using systems biology approaches

Stechow, L. von

IDENTIFICATION OF METABOLIC PATHWAYS IN THE DNA DAMAGE RESPONSE IN PLURIPOTENT STEM CELLS

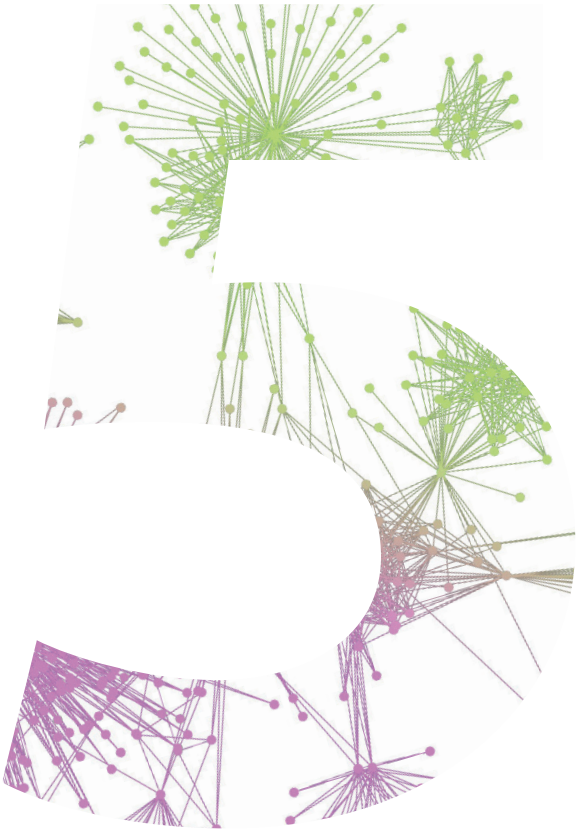

MANUSCRIPT SUBMITTED

Louise von Stechow*, Ainhoa Ruiz-Aracama*, Bob van de Water, Ad Peijnenburg, Erik HJ Danen, Arjen Lommen

ABSTRACT

DNA damage triggers the activation of an orchestrated signaling network to arrest the cell cycle and repair the lesions or, in case of damage beyond repair, eliminate affected cells. Failure to properly balance the various aspects of this DNA damage response (DDR) in stem cells contributes to ageing and cancer. We and others have shown that treatment of pluripotent stem cells with chemotherapeutic agents, such as cisplatin causes a plethora of transcriptional and post-translational alterations that determine the outcome of the DDR. Here, we performed metabolic profiling by mass spectrometry of embryonic stem (ES) cells treated for different time periods with cisplatin. Integration of metabolomics with transcriptomics data connected cisplatin-regulated metabolites with regulated metabolic enzymes and identified enriched metabolic pathways. These included nucleotide metabolism, urea cycle and arginine and proline metabolism, and a group of metabolic pathways that clustered around the metabolite S-adenosylmethionine, which is a hub for methylation and transsulfuration reactions and polyamine metabolism. A number of the differentially regulated metabolic enzymes were identified as target genes of the transcription factor p53, pointing to p53-mediated alterations in metabolism in response to genotoxic stress. Altogether, our findings reveal interconnecting metabolic pathways that serve as signaling modules in the DDR.

INTRODUCTION

Metabolic changes are associated with a number of complex diseases, including cancer, diabetes and neurological disorders. Often, changes in the abundance of small metabolites are linked to changes in the expression or activity of metabolic enzymes or the complete rewiring of metabolic pathways, as seen for cancer cells, which frequently switch their energy production to aerobic glycolysis (known as Warburg effect) and develop a glutamine addiction [1; 2; 3]. Indeed, mutations in a number of metabolic enzymes were recently related to inherited cancer syndromes [3]. This link between metabolism and disease suggests that metabolomics may be used to identify biomarkers suitable for non-invasive methods to determine disease state, treatment and toxic responses [4].

Changes in metabolism may be linked to stress responses, such as genotoxic stress. Irradiation or chemotherapeutic treatment alters the abundance of metabolites, including for example choline-containing compounds, lipids and several amino acids in cancer cell lines [5; 6]. Interestingly, metabolites excreted by cancer-associated stromal cells can modulate chemosensitivity of cancer cells in a paracrine manner [7]. Recently, the NCI60 panel of tumor cells lines was used to correlate treatment response to platinum drugs with baseline metabolic pathways extracted from metabolomics and transcriptomics [8]. However, integrated approaches aimed at unraveling perturbation of metabolic pathways in response to therapy are currently lacking.

The ability of cells to recognize and respond to DNA damage is of vital importance for the maintenance of an intact genome. The DNA crosslinking drug cisplatin is used as common treatment for various solid tumors, e.g. ovarian, non-small-cell lung, head and neck, bladder, colorectal and testicular cancer. Despite initial good responses to therapy, patients often develop resistance to cisplatin treatment and toxicity to healthy tissues (including neuro- and renal as well as gastric toxicity) limits the therapeutic window [9]. Next to direct DNA damage, cisplatin also induces non-genotoxic perturbations, such as oxidative stress by shifting the redox balance through binding to nucleophilic molecules; and ER stress, which has been shown to kill enucleated cells [10; 11].

Cancer cells typically have disabled crucial DDR signaling routes and often rewire metabolic pathways [3; 12]. We recently unraveled the DDR signaling network in mouse embryonic stem (ES) cells through integration of functional genomics, phosphoproteomics, and transcriptomics [13; 14]. ES cells show robust DNA damage-induced apoptosis, but have several features that can be extrapolated to cancer cells, such as the lack of G1/S-checkpoint after DNA damage, expression of marker genes (e.g. c-Myc), and a high proliferation rate [15; 16]. Here, we integrated metabolomics and transcriptomics datasets to explore alterations in metabolic pathways in response to genotoxic stress in pluripotent stem cells.

RESULTS

Cisplatin-induced changes on the metabolome of embryonic stem cells

General considerations - To explore intracellular metabolic changes in response to genotoxic stress in pluripotent stem cells, ES cells were treated with a sub-lethal dose of 5 μM cisplatin for 4 h and 8 h and lysates were prepared for metabolomics analysis (Fig S1A). At 8 h cells began to accumulate in the S/G2 phase of the cell cycle but viability was not significantly affected at these early timepoints while analysis of parallel control plates at later time points confirmed induction of apoptosis by this concentration of cisplatin (Fig Sfig1B-D). Apolar and polar fractions were collected and used for 1H-NMR and U-HPLC-Orbitrap-MS analysis, respectively. To assess whether data normalization was required to correct for potential differences in cell numbers 1H-NMR data on the apolar fraction of control and cisplatin treated ES cells at both time points were analyzed. Since no significant differences (ANOVA $p<0.01$) in phospholipid content or other apolar metabolites were detected (examples of overlaid spectra are given in Fig S2), normalization of metabolite data to correct for cell numbers was not required. Finally, PCA demonstrated excellent reproducibility for all 5 biological replicates within each treatment and exposure time group (Fig S3).

Identification of metabolites significantly affected by cisplatin - Polar fractions of control- and cisplatin-treated samples were compared for each time point independently. Masses were identified that significantly contributed to the observed separation between treatments at the different time points (Table S1). At 4 h, metabolites that were differentially regulated between control and cisplatin treated samples were mainly involved in methionine degradation pathways (including transmethylation, transsulfuration/glutathione synthesis), as well as polyamine synthesis and catabolism, urea cycle, proline and arginine metabolism, and nucleotide metabolism (Fig 1A). Furthermore, we detected increased levels of the metabolite N-acetyl-aspartyl-glutamic acid (NAAG), a common neuropeptide and its precursor N-acetyl-L-aspartate (NAA) [23] (Fig 1A). After 8 h of cisplatin treatment, levels of reduced glutathione and proline remained increased, while other differentially regulated metabolites were mainly involved in nucleotide metabolism (Fig 1 B, Table S1).

Expression of metabolic enzymes significantly affected by cisplatin

In parallel to metabolomics, transcriptomics analysis was performed to determine cisplatin-induced changes in metabolic enzymes at 8 h. Cytoscape and IPA-based pathway analysis led to the identification of a list of 144 metabolism-related enzymes (Table S2, Fig 2A). A large proportion of these metabolic enzymes were involved in lipid metabolism; inositol phosphate metabolism (mostly myo-Inositol), glycerophospholipid and sphingolipid metabolism. We furthermore detected changes in the mRNA levels of metabolic enzymes that are involved in sugar and fatty acid metabolism (Fig 2A). Next to those, a number of differentially-regulated metabolic enzymes correlated with the

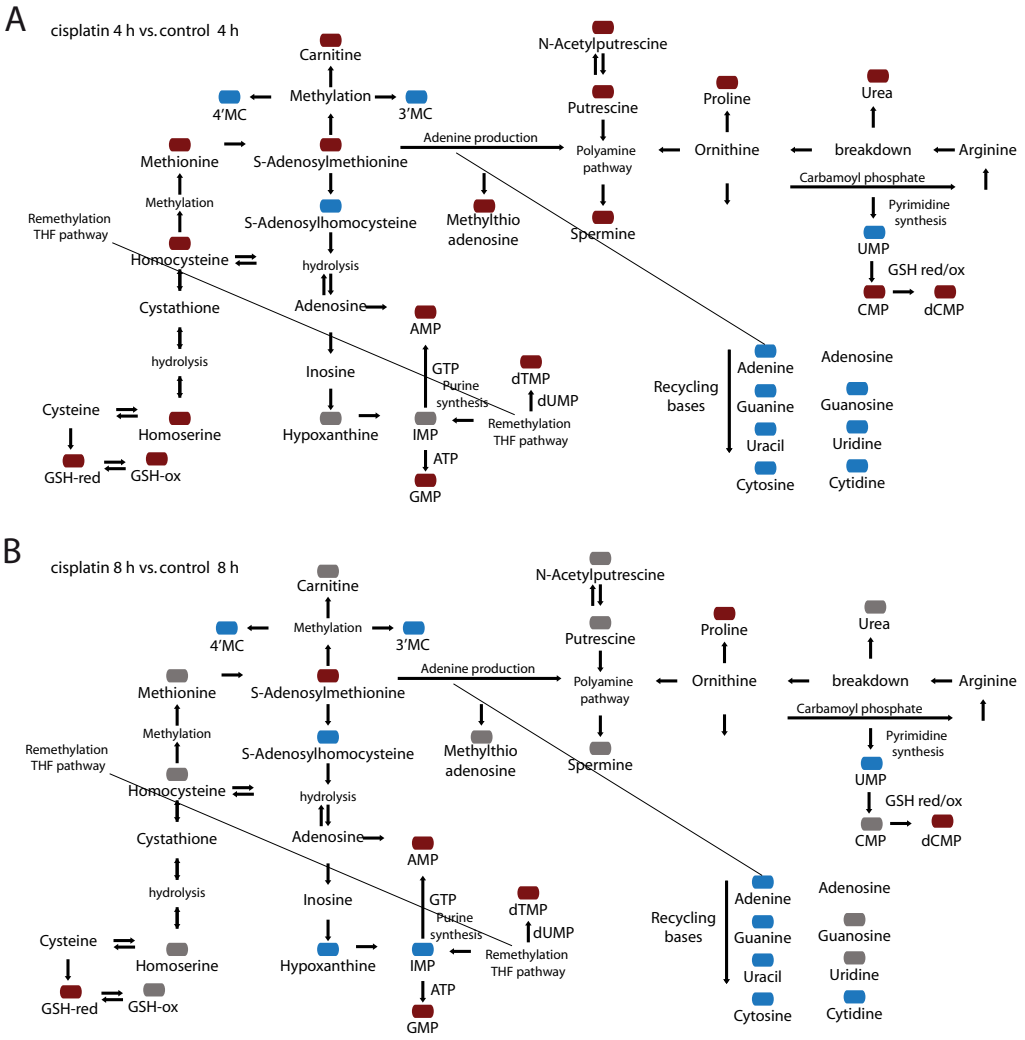

Figure 1. Network of differentially regulated metabolites. Red, Blue and Grey boxes indicate metabolites (mean of 5 replicates) upregulated, downregulated, and unchanged in cisplatin treatment, respectively (ANOVA $p<0.01$ and fold change 1.1); metabolites without a box were not detected. (A) Results after 4 h. (B) Results after 8 h.

metabolic pathways, which had been identified based on the changes in metabolite levels, including urea cycle and arginine/ proline metabolism, polyamine metabolism and nucleotide metabolism (Fig 2A). Interestingly, several of the cisplatin-regulated metabolic enzymes were identified as target genes of the transcription factor p53 (Fig 2B). p53 target genes implicated in lipid metabolism were commonly suppressed while p53 target genes encoding enzymes functioning in amino acid or nucleotide metabolism were mostly enhanced.

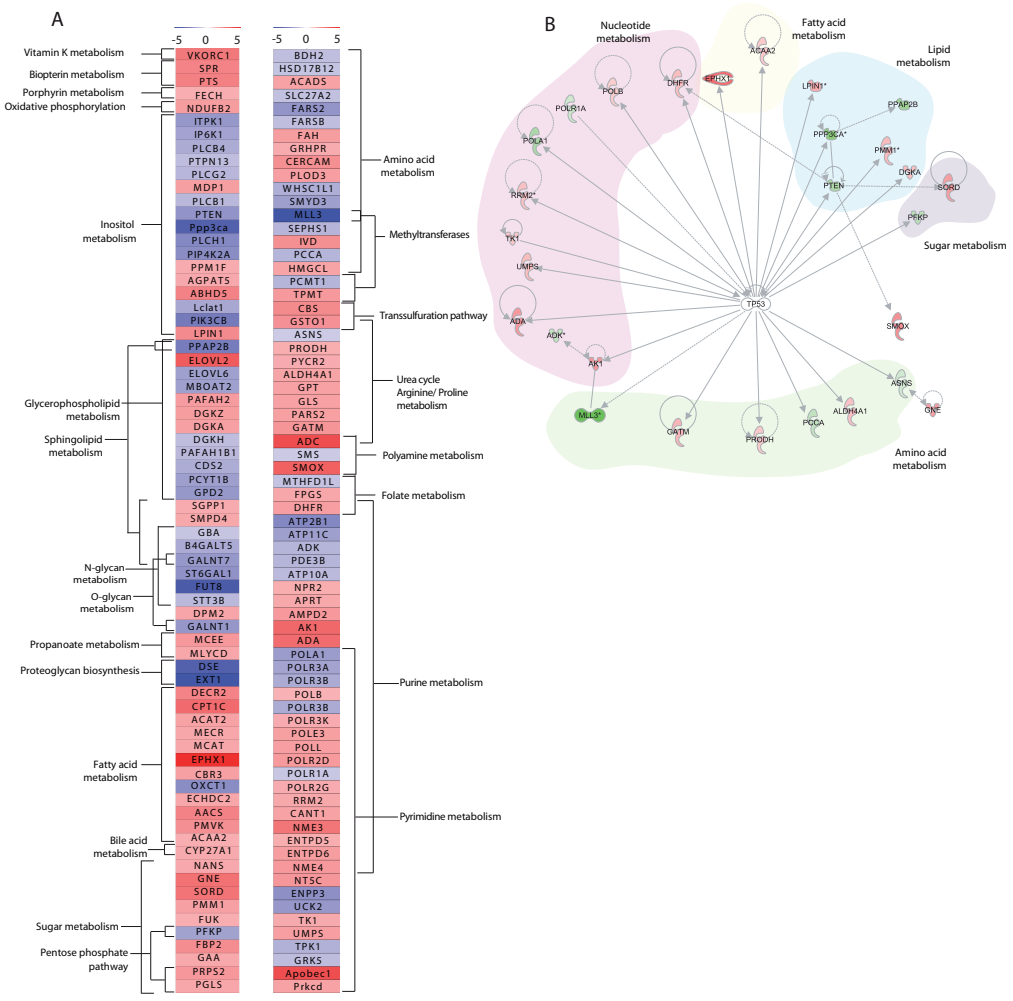

Figure 2. Differentially regulated metabolic enzymes. (A) Heatmap indicating metabolic enzymes obtained from Cytoscape metabolic signaling network (FigS 4, highlighted in blue; TableS 2), differentially regulated after 8 h of cisplatin treatment and enriched metabolic pathways within the dataset. (B) Regulation of metabolic enzymes by the transcription factor p53 obtained with Ingenuity pathway analysis.

Identification of affected metabolic pathways through integration of metabolomics and transcriptomics

Identified changes in metabolites and metabolic enzymes were combined to derive integrated signaling networks. For this, 144 regulated enzymes and 35 regulated metabolites were imported in IPA and Metscape to form an integrated metabolic signaling network (Fig 3; Fig S4). Clusters of significantly enriched metabolic pathways were identified based on the criteria [>3 affected molecules including at least 1 affected metabolite and 1 affected enzyme]. Lipid metabolism, despite the observed changes in expression of several enzymes in this process (Fig 2A; Table S2), was not selected due to the absence of information on affected metabolites. The sample

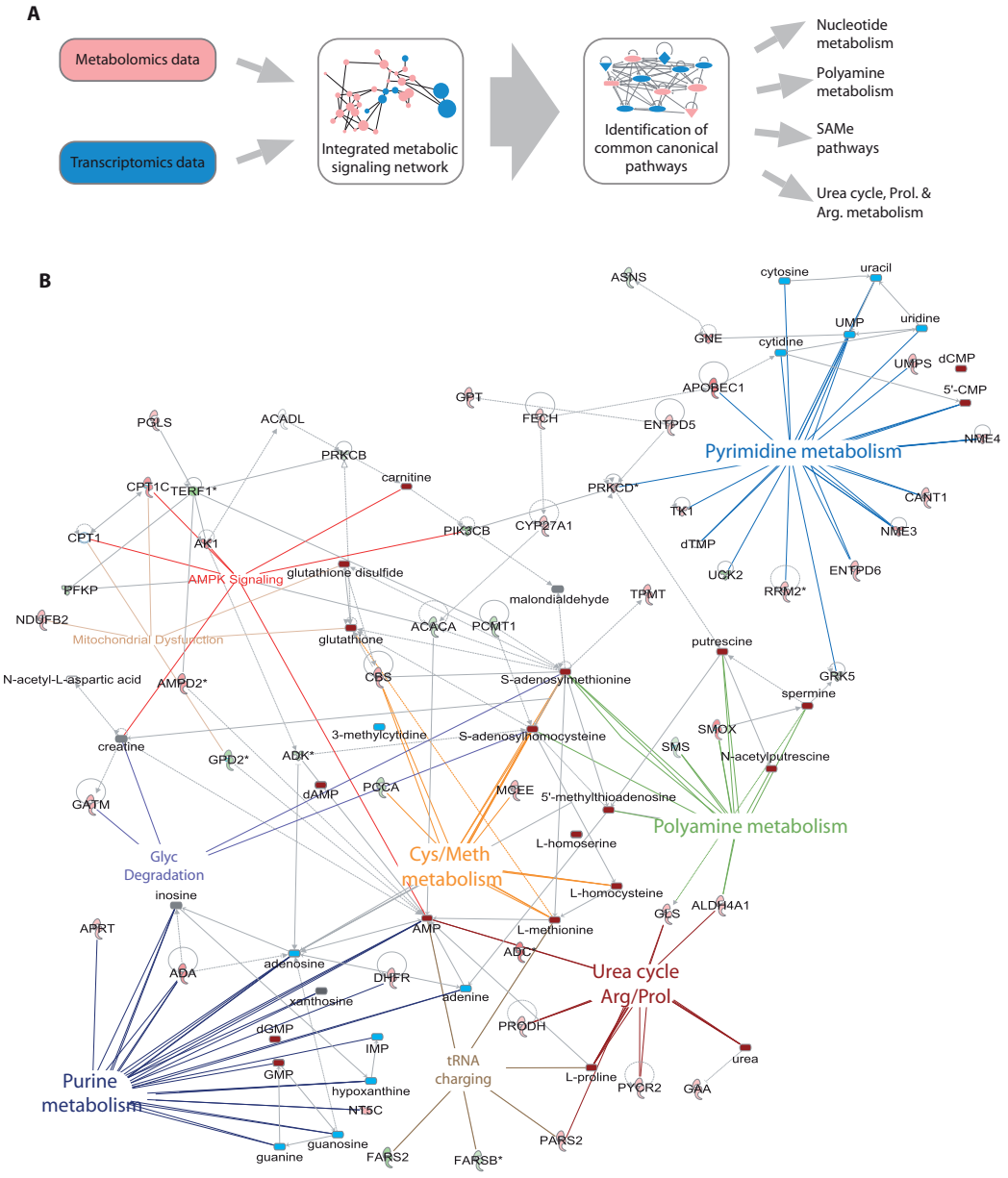

Figure 3. Integrated signaling network. (A) Schematic representation of metabolomics and transcriptomics data integration leading to identification of common signaling networks related to nucleotide metabolism, SAMe pathways, polyamine pathways and urea cycle, and arginine & proline metabolism. (B) Integrated signaling network of metabolic enzymes and metabolites obtained with Ingenuity pathway analysis. Clusters of significantly enriched canonical pathways and related enzymes and metabolites are highlighted. Upregulated enzymes in green, downregulated enzymes in red. Upregulated metabolites in dark red, downregulated metabolites in blue.

analysis methodology (NMR) used here for the apolar (lipid) fraction does not have the required resolution for detection of metabolites on the individual species level (such as for instance PIP3 etc). Networks included a purine and a pyrimidine metabolism cluster, a cluster of S-adenosylmethionine (SAMe)-related pathways, a polyamine synthesis cluster, and a urea cycle cluster, featuring pathways related to the metabolism of proline, arginine and citrulline (Fig 3, 4, 5, Fig S5, 6).

At 4 h of cisplatin treatment many metabolites linked to SAMe-related pathways were increased (Fig 1,3,4). SAMe is the methyl donor in methylation of DNA, RNA and methylation of lysine during biosynthesis of carnitine [24]. We detected cisplatin-induced changes in the levels of the RNA nucleosides 3-methylcytidine, 4-methylcytidine, and of carnitine, as well as changes in mRNA levels of the methyltransferases MLL3, PCMT1 and TPMT (Fig 2A, Fig 3). We reinvestigated the list of differentially regulated genes and identified regulation of several other methylation enzymes that had been missed by IPA and Metscape analysis, including histone methyltransferases and demethlyases as well as RNA methyltransferases (Fig S7A). This additional list included the RNA methyltransferase METLL6, which has been correlated to cisplatin sensitivity in lung cancer patients [25]. SAMe is a critical hub between trans-sulfuration, polyamine synthesis, and the folate cycle [24]. Multiple enzymes and metabolites in these pathways were significantly regulated by cisplatin (Fig 4). This included an increase in cystathionine-beta-synthase (CBS), an enzyme that is critical for the conversion of homocysteine to

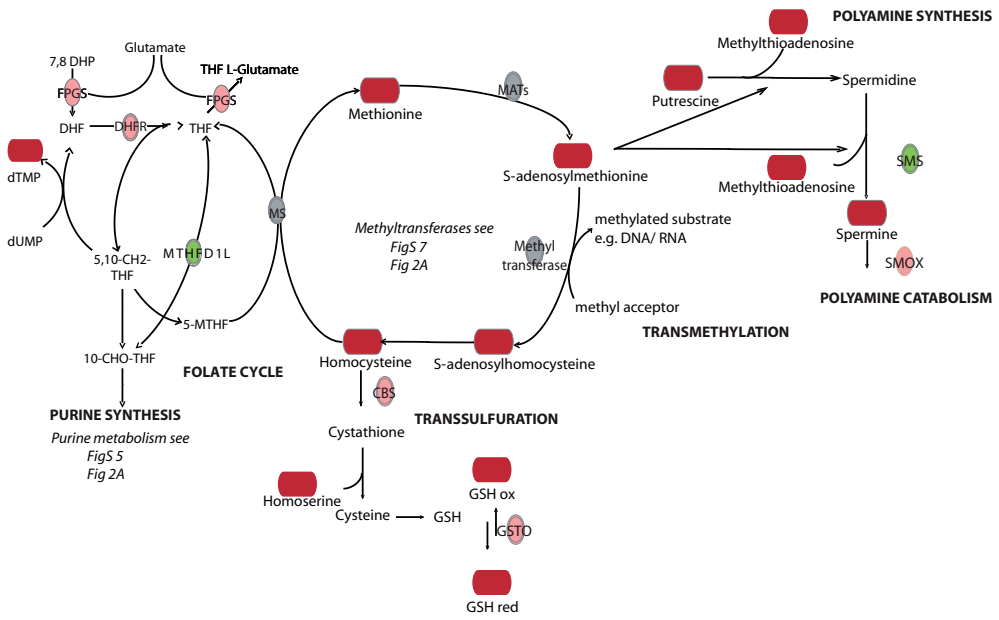

Figure 4. SAMe centered pathways. Upregulated enzymes in green, downregulated enzymes in red. Upregulated metabolites in dark red, downregulated metabolites in blue.

cystathione [24]. Cystathione is a precursor for glutathione and levels of oxidized and reduced glutathione were increased after 4 h of cisplatin treatment, while after 8 h only the reduced form persisted (Fig 1, Table S1). Enzymes related to tetrahydrofolate (THF) synthesis, which is a crucial part of the folate cycle were also affected. THF is not only involved in transmethylation, but is also crucial to pyrimidine and purine synthesis. This included upregulation of FPGS and DHFR, which are directly involved in THF synthesis, and downregulation of MTHFD1L, which is involved in the ATP/ADP-dependent interconversion of 10-formyl-THF (needed for purine synthesis) (Fig 4).

A cluster of reactions related to polyamine synthesis and catabolism were identified based on cisplatin-regulation of enzymes and metabolites (Fig 4,5). After 4 h of cisplatin treatment we identified increased levels of the polyamine metabolites spermine and its precursor putrescine. At 8 h the concentrations were normalized again, while at the same time spermine synthase (SMS) mRNA levels were reduced and spermine oxidase (SMOX) mRNA levels were increased. In addition, changes in metabolites and enzymes related to urea cycle and proline/ arginine metabolism were identified (Fig 1,5). Arginine catabolism appeared to be enhanced even though we did not observe transcriptional changes in superoxide dismutase or NO-synthase. ADC was found to be strongly increased, potentially resulting in a higher conversion of arginine to agmatine, which itself is an inhibitor of NO-synthase. Moreover, expression of GATM, which forms a creatine precursor from arginine and glycine was enhanced (Fig 5) [26]. Enhanced levels

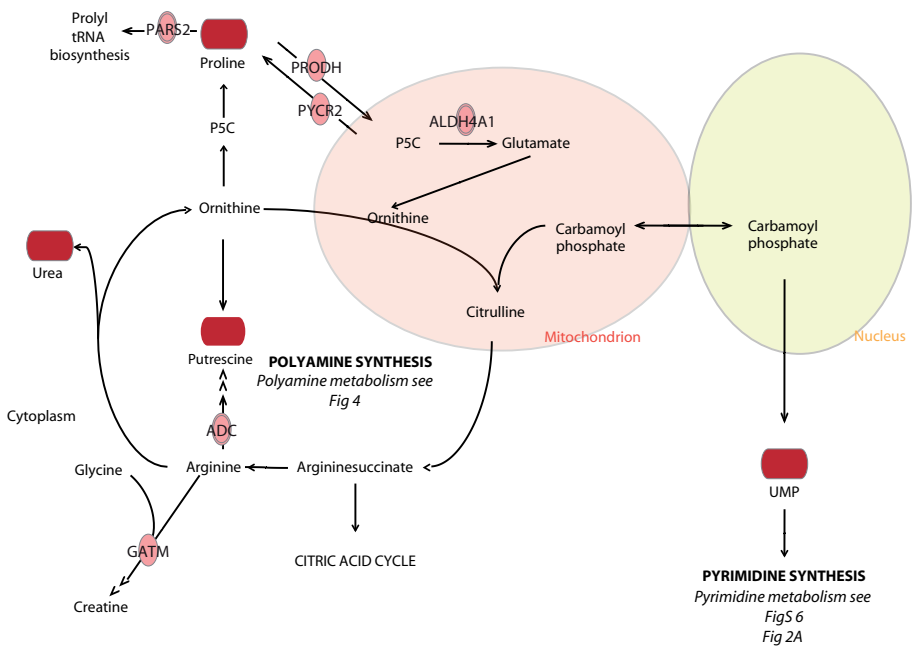

Figure 5. Urea cycle and the metabolism of arginine and proline. Upregulated enzymes in green, downregulated enzymes in red. Upregulated metabolites in dark red, downregulated metabolites in blue.

of metabolic products of arginine catabolism such as urea, putrescine (and spermine) and proline were also detected [26] (Fig 5). Next to increased proline levels at 4 h and 8 h of treatment enzymes involved in reduction of P5C to proline (PYCR2), as well as proline breakdown (PRODH, Aldh4a1) were up-regulated [27]. Notably, IPA analysis identified PRODH, Aldh4a1, and GATM as known p53 target genes [28; 29] (Fig 2A).

Since many of the enzymes and metabolites have been previously implicated in anti- or prooxidant function (e.g. glutathione, methionine, proline, PRODH, SMOX) we tested whether cisplatin treatment, at the time points of our analysis, led to an increase in reactive oxygen species (ROS) formation. However, while hydrogen peroxide led to a strong increase in ROS levels, no significant increase in intracellular ROS levels were detected by cisplatin treatment, at any of the studied time points (FigS 7B).

Lastly, several metabolites and metabolic enzymes involved in purine/pyrimidine metabolism were significantly regulated by cisplatin treatment (Fig 1,2,3; Fig S5,6). These were implicated in de novo synthesis and salvage pathways (Fig S5,6) and included a group of enzymes encoded by genes that were identified in IPA as p53 targets. For instance, DNA polymerase β and RRM2 were upregulated while the catalytic subunit of the replicative B-family DNA polymerase α was downregulated [30; 31] (Fig 2B).

DISCUSSION

The DDR activates, in a damage-specific fashion, the appropriate enzyme complexes dedicated to the repair of a variety of DNA lesions. It is critical that the DDR is integrated with ongoing cellular activities, including cell cycle progression, transcription, and translation. In the case of severe damage it is important to arrest the cell cycle, prevent aberrant transcription and translation, preserve energy, and, if damage is beyond repair, to activate cell death mechanisms. This is particularly relevant in stem cells where defective DDR signaling can have major impacts on ageing and cancer [32; 33]. Clearly, the DDR extends into all vital cellular processes. Our current study identifies alterations in metabolic pathways that are likewise controlled by the DDR in pluripotent stem cells.

It must be noted that the metabolomics profiles generated here provide a snapshot of the total dynamic regulation of metabolism under standard and stressed conditions This is for instance due to technical limitations that exclude certain metabolites from the analysis, the labile nature of some metabolites, and the absence of information on flux. Nevertheless, the strong reproducibility of the data (typically a bottleneck in metabolomics) and the connections with affected metabolic enzymes provide high-confidence data on the metabolic response of ES cells to genotoxic insult. Interestingly, a number of metabolic enzymes we find to be transcriptionally modified by cisplatin are target genes of the key DDR transcriptional regulator, p53. This is in agreement with our recent finding that p53 is a major DDR signaling hub in ES cells [13]. Moreover, the integration of transcriptionally regulated metabolic enzymes and significantly affected

metabolites allows identification of integrated metabolic networks that are responsive to genotoxic stress. These cluster in pathways centered on purine/pyrimidine metabolism, SAMe-related pathways, polyamine synthesis, and the urea cycle.

Changes in methylation pathways

Our analysis shows an increase in SAMe-related metabolites in response to cisplatin treatment. SAMe is formed from methionine and ATP with the help of methionine adenosyltransferases (MATs) and functions as a general methyl donor in almost all cellular methylation reactions [24]. Methylation patterns (especially those of DNA) change during embryonic development and neoplastic transformation and can be affected by genotoxic stress [34]. RNA-methylation has been associated with structural features, RNA stability and function (e.g. tRNA codon specificity) [35]. Mammalian cells lack the necessary kinases to phosphorylate modified nucleosides into nucleoside triphosphate, which prevents their recycling and incorporation in mRNA [36]. Instead, modified nucleosides are excreted. Enhanced urinary levels of modified RNA nucleosides, including 3-methylcytidine have been suggested as a potential biomarker for certain cancers [37; 38]. We detect changes in the expression of RNA- but not DNA-methyl transferases and decreased levels of methylated RNA nucleosides in response to cisplatin treatment, including 3- and 4-methylcytidine.

Changes in transsulfuration pathways and folate cycle

After methyl transfer SAMe is converted into S-adenosylhomocysteine (SAH), which in turn is hydrolyzed to form adenosine and homocysteine. Homocysteine, can be either reduced to cysteine, which functions as a crucial precursor for glutathione (Transsulfuration pathway), or be remethylated to methionine (Folate cycle) [24]. Our integrated metabolic network associated with SAMe points to changes in these pathways. Glutathione - a cytoprotective compound - has been reported to chelate cisplatin and to play a role in copper transporter mediated cisplatin efflux. Furthermore, glutathione has a function in cellular redox regulation and can act as a protective agent against cisplatin-induced oxidative stress [39; 40; 41]. In accordance with this, GSTO1, a member of the highly conserved omega class of glutathione transferases with dehydroascorbate reductase activity, which has been implicated in resistance to various genotoxic drugs and irradiation, shows increased levels after cisplatin treatment [42; 43]. In addition, cisplatin treatment causes changes in the levels of enzymes associated with folate synthesis and the folate cycle although altered levels of relevant metabolites are not seen. Expression of DHFR and FGPS is upregulated whereas MTHFD1L is decreased, which could provide a connection to the observed changes in purine metabolism through ATP/ADP-dependent interconversion of 10-formyl-THF [44]. Interestingly, antifolates, such as the DHFR interactor methotrexate are used as antineoplastic agents [45].

Changes in polyamine related pathways

SAMe serves as a precursor for elongation of putrescine to spermidine and from there to spermine [24]. Both putrescine and spermine levels are enhanced in cisplatin-treated cells at 4 h. The increase of putrescine, which can be derived from ornithine, could also be explained by enhanced expression of ADC, an arginine decarboxylase that converts arginine to agmatine, a precursor of putrescine. Spermine is the substrate for SMOX, an enzyme that is upregulated at 8 h by cisplatin and catalyzes the breakdown of spermine to spermidine, 3-aminopropanal, and H_2O_2. Platinum drugs have already been shown to regulate enzymes involved in polyamine catabolism, including spermine N1-acetyltransferase (which is not seen in our study) and SMOX [46; 47]. Moreover, SMOX-produced H_2O_2 is considered a major source of oxidative stress after induction of polyamine catabolism [47]. Therefore it appears that the initially increased levels of polyamines could later be levelled out by oxidation potentially leading to an increased production of H_2O_2.

Changes in proline/ arginine metabolism and urea cycle

We show that cisplatin induces substantial changes in metabolites and enzymes related to urea cycle and proline/ arginine metabolism including an apparent increase in arginine catabolism. Arginine, proline, glutamate and ornithine are all interconvertable provided that glutamine is available as a precursor of carbamoyl phosphate. This metabolism is the basis for synthesis of nitrogen-containing compounds such as ureum, putrescine, agmatine, creatine and even nitrogen oxide and is furthermore crucial for pyrimidine synthesis. Interestingly, changes in pyrimidine metabolites are seen in response to cisplatin treatment, including an increase in the pyrimidine synthesis precursor, UMP [26; 48].

Effects of cisplatin on purine/pyrimidine/nucleotide metabolism

Cisplatin affects DNA replication and transcription by causing inter- and intrastrand crosslinks and it can bind free nucleotides. Our integrated networks indicate that pathways potentially involved in DNA metabolism, such as purine/pyrimidine and nucleoside/nucleotide metabolism are significantly increased, including both *de novo* synthesis and salvage pathways. Notably, interpretation of changes in nucleotide metabolism is complicated by the fact that nucleotides, next to serving as building blocks of DNA and RNA, are involved in a great number of cellular signaling functions, as well as energy metabolism [49]. This cluster may be affected by DNA damage in a p53-dependent manner: affected polymerases and enzymes involved in DNA synthesis and repair are regulated by p53.

Possible cisplatin-ROS related metabolism

Different studies have reported cisplatin-induced oxidative stress but the relative contribution of this to cisplatin cytotoxicity is unclear. Cisplatin can cause oxidative stress by depleting cellular antioxidant defenses due to its binding to nucleophilic

molecules such as glutathione, methionine or cysteine-rich proteins [11]. Furthermore, cisplatin-induced (DDR) signaling processes might cause secondary oxidative stress. The cisplatin-regulated metabolic pathways discussed above provide a number of links to generation of oxidative stress. For instance, a generally increased arginine catabolism may lead to nitrogen oxide formation through NO-synthase, which has been associated with ROS, while an increase in SMOX can lead to H_2O_2 production [47]. Notably, we do not detect elevated ROS at the timepoints and cisplatin concentrations used in our study (whereas H_2O_2 strongly induces ROS, as expected). This may indicate absence of cisplatin-induced ROS production or effective scavenging of ROS in ES cells. The enhanced levels of glutathione, methionine and proline metabolites may point to the latter explanation and indicate that ES cells cope with cisplatin-induced oxidative stress [41; 50]. However, the fact that the ratio reduced versus oxidized glutathione is slightly elevated in cisplatin-treated cells, argues against glutathione-mediated ROS-scavenging.

CONCLUSIONS

By integrating metabolomics and transcriptomics analyses of cisplatin-treated ES cells, we have identified metabolic pathways that are significantly affected by the treatment with this genotoxic compound. Part of this metabolic response is mediated by p53, in agreement with its central role in the DDR. This includes for instance DNA damage repair-related nucleotide metabolism enzymes (e.g. RRM2) and amino acid catabolic enzymes (e.g. PRODH, ALDH4a1, GATM). Changes in individual metabolic enzymes or metabolites have been reported by others to be responsive to genotoxic stress and/or associated with sensitivity to genotoxic therapy in cancer cells. This holds true for instance for GSTO1, METLL6, PRODH, and SMOX enzymes and metabolites such as carnitine, methionine, and glutathione. However, our current study for the first time provides the signaling networks that integrate these events within the metabolic branch of the DDR.

MATERIAL AND METHODS

Cell culture and materials

HM1 mouse ES cells derived from OLA/129 genetic background (provided by Dr. Klaus Willecke, University of Bonn GE) were maintained under feeder free conditions in GMEM medium containing 10% FBS, $5x10^5$ U mouse recombinant leukemia inhibitory factor (LIF; PAA), 25 U/ml penicillin, and 25 µg/ml streptomycin. For metabolomics analysis and micro-arrays ES cells were used at passage 22. Cells were confirmed to be mycoplasma-free using the Mycosensor kit from Stratagene. The DNA cross-

linkers cisplatin (cisplatin; Cis-PtCl2(NH3)2) was provided by the Pharmacy unit of University Hospital, Leiden NL. Ammonium acetate (NH4Ac), sodium chloride (NaCl) and deuterated chloroform (CDCl3) were obtained from Merck (Darmstadt, Germany); methanol (MeOH) and acetone from Biosolve (Valkenswaard, The Netherlands). All chemicals and solvents were purchased in the highest purity available. Ultra-pure water was obtained using the PureLab equipment from Rossmark (Ede, The Netherlands).

Cell viability, apoptosis and cell cycle analysis

To monitor cisplatin induced cell killing, a cell viability assay using ATPlite 1Step kit (Perkin Elmer) was performed according to the manufacturer's instructions followed by luminescence measurement using a plate reader. For cell cycle and apoptosis analysis cells were exposed to vehicle (PBS) or cisplatin for 8 h or 24 h. Floating and attached cells were pooled and fixed in 80% ethanol overnight. Cells were stained using PBS EDTA containing 7.5 mM propidium iodine and 40 mg/ml RNAseA and measured by flow cytometry (FACSCanto II; Becton Dickinson). The number of cells in the different cell cycle fractions (and in sub G0/G1 for apoptotic cells), as seen in FigS 1 was calculated using the BD FACSDiva software.

Metabolomics – sample preparation

HM1 ES cells were treated with 5 μM cisplatin or vehicle control for 4 h and 8 h followed by lysis and fractionation as described [17]. Five independent biological replicates were examined in each experiment. Metabolomics analysis was performed on the apolar fraction, containing the membranes and intracellular lipids, and the polar fraction containing the polar and semi-polar intracellular metabolites. In short, the pellet containing the apolar metabolites, was resuspended in 1 M NH4Ac, freeze-dried, extracted with CDCl3, and the organic solvent was evaporated under N2 flow. The dried extract was dissolved in 1 ml of CDCl3, 0.6 ml of which was used for NMR analysis. The supernatant containing the polar intracellular metabolites was freeze-dried, resuspended in 1 ml MeOH, dried with N2, and re-suspended in 50% MeOH/ 50% H_2O ultra-pure water. To remove gelatin derived from the adhesive coating used for the ES cell cultures, this sample was consecutively mixed with cold acetone, incubated for 10 min at 4˚C and centrifuged 15 min at 13,000 x g at 4˚C. The supernatant was collected and dried under nitrogen for further analysis.

Metabolomics – measurements

The apolar samples were analyzed by 1H-NMR. The 1H-NMR spectra were recorded at 400.13 MHz at 300.0 (± 0.02) K on a Bruker Avance 400 narrow bore using a 5.0-mm probe. The spectrometer settings were the same as described previously [17]. The polar samples were analyzed by ultra-high performance liquid chromatography (U-HPLC)-Orbitrap-MS. For this the samples were diluted twice with H_2O and formic acid was added to a final concentration of 0.1%. The injection sequence was randomized as described [18]. U-HPLC was performed on a U-HPLC Accela system (Thermo Fisher Scientific, San

Jose, CA, USA), with a 150 mm × 2.1 mm UPLC BEH-C18 column with 1.7 µm particles (Waters). Chromatographic conditions were as described [17]. The U-HPLC was directly interfaced to a single stage Orbitrap mass spectrometer (Exactive, Thermo Fisher Scientific). Settings of the Orbitrap mass spectrometer are provided (Suppl. Material 1). Data were recorded using Xcalibur software version 2.1.0.1139 (Thermo Fisher Scientific). When identification of mass peaks was needed, samples were subjected to LC-nanomate-Orbitrap-MS analysis using chromatography conditions as described above. These identification procedures are as previously described [17].

Metabolomics - data analysis

NMR data analysis of apolar samples: A method for normalization of data using phospholipid signals in apolar samples was accessed as previously described [17]. The NMR data were pre-processed and aligned as described using a for Windows updated version of in-house developed software [19]. Based on equal phospholipid content, normalization of data was not required (see Results section). Subsequently, the spreadsheet containing aligned data of the apolar samples was subjected to statistical analysis using Genemaths XT (http://www.applied-maths.com/genemaths/genemaths.htm). Standard initial analysis entailed performing a 2Log transformation and a principal component analysis (PCA) (average of rows and columns subtracted). This was followed by a 2Log transformation, a pre-selection of variables using an ANOVA ($p<0.01$), followed by a PCA (average of rows and columns subtracted). The grouping in the ANOVA was on the replicates (n=5) per treatment (control and 5 µM cisplatin) for each timepoint (4 and 8 hours) creating 4 groups with 5 replicates or on the treatments, creating 2 groups of 10 replicates.

LC-MS data analysis of polar samples: U-HPLC-Orbitrap-MS data were pre-processed, mass corrected to sub-ppm precision [19] and aligned using MetAlign (http://www.metalign.nl) [20]. In short, this software performs a baseline correction, accurate mass calculation, data smoothing, and noise reduction, followed by alignment between chromatograms. Since the NMR data on apolar samples did not indicate a need for normalization (see Results) and the polar samples were derived from the same cell cultures no normalization was applied on U-HPLC-Orbitrap-MS data. The generated spreadsheet of the dataset was subjected to statistical analysis using Genemaths XT. Standard initial analysis entailed performing a 2Log transformation and a PCA (average of rows and columns subtracted). This was followed by a 2Log transformation, a pre-selection of variables using an ANOVA ($p<0.01$), followed by a PCA (average of rows and columns subtracted). The grouping in the ANOVA was: on the replicates for each time point and treatment (4 groups with 5 replicates), per treatment (2 groups of 10 replicates), on the control samples at both time points (2 groups of 5 replicates), as well as per treatment at each time point (2 groups of 5 replicates at 4 h and 2 groups of 5 replicates at 8 h). The peak loadings responsible for the separation in the different PCAs were selected and exported as described [20]. Only those signals with intensity

higher than 5 times noise and a fold change higher than 1.2 were taken as candidates for further identification.

Identification of metabolites: To facilitate further analysis and identification of the selected signals, GM2MS, an application of MetAlign that re-creates "new chromatograms" only containing the peaks exported from the PCA selection, was used [20]. Polar metabolites were afterwards identified with commercially available standards, using previous acquired identification information [17], with FT-MS/MS analysis (using the LC-nanomate-Orbitrap-MS method described above), and using databases such as the HMDB [http://www.hmdb.ca/] (see TableS 1 for the identified metabolites).

Transcriptomics analysis and integration of metabolomics and transcriptomics data

Transcriptional microarray data have been published [13] and are available from ArrayExpress. The 2269 genes whose expression differed significantly (parametric $p<0.0005$) between control ES cells and ES cells treated for 8 hours with 10 μM cisplatin were used as input in Ingenuity pathway analysis (IPA) or the cytoscape plug-in Metscape to identify metabolic enzymes [21; 22]. Transcriptional heatmaps were obtained using Multiple Array Viewer (MEV) software. Differentially expressed genes encoding metabolic enzymes and the metabolites that were differentially regulated at 4 h or 8 h ($p<0.01$) were imported in IPA and Metscape to form integrated metabolic signaling networks.

ROS formation assay

For probing intracellular ROS, cells were cultured in μClear 96 well plates to 70% confluence. Cells were washed twice with PBS and incubated for 1 h with 40 μM 5-(and-6)-Carboxy-2',7'-Dichlorofluorescein Diacetate (DCF-DA, Invitrogen) in phenol-red free culture medium. After washing with PBS, cells were exposed to 5 μM cisplatin or 250 μM Hydrogen peroxide (H_2O_2) in the presence or absence of 10 mM of the ROS scavenger N-acetylcysteine (NAC). Fluorescence was measured at different time points after exposure using a plate reader.

ACKNOWLEDGEMENTS

This work was supported by the Netherlands Genomics Initiative /Netherlands Organization for Scientific Research (NWO): nr 050-060-510.

REFERENCES

1. Patti, G. J., Yanes, O. & Siuzdak, G. (2012). Innovation: Metabolomics: the apogee of the omics trilogy. Nat Rev Mol Cell Biol 13, 263-9.

2. Suhre, K., Shin, S. Y., Petersen, A. K., Mohney, R. P., Meredith, D., Wagele, B., Altmaier, E., Deloukas, P., Erdmann, J., Grundberg, E., Hammond, C. J., de Angelis, M. H., Kastenmuller, G., Kottgen, A., Kronenberg, F., Mangino, M., Meisinger, C., Meitinger, T., Mewes, H. W., Milburn, M. V., Prehn, C., Raffler, J., Ried, J. S., Romisch-Margl, W., Samani, N. J., Small, K. S., Wichmann, H. E., Zhai, G., Illig, T., Spector, T. D., Adamski, J., Soranzo, N. & Gieger, C. (2011). Human metabolic individuality in biomedical and pharmaceutical research. Nature 477, 54-60.

3. Dang, C. V. (2012). Links between metabolism and cancer. Genes Dev 26, 877-90.

4. Zhang, G. F., Sadhukhan, S., Tochtrop, G. P. & Brunengraber, H. (2011). Metabolomics, pathway regulation, and pathway discovery. J Biol Chem 286, 23631-5.

5. Duarte, I. F., Lamego, I., Marques, J., Marques, M. P., Blaise, B. J. & Gil, A. M. (2010). Nuclear magnetic resonance (NMR) study of the effect of cisplatin on the metabolic profile of MG-63 osteosarcoma cells. J Proteome Res 9, 5877-86.

6. Cano, K. E., Li, Y. J. & Chen, Y. (2010). NMR metabolomic profiling reveals new roles of SUMOylation in DNA damage response. J Proteome Res 9, 5382-8.

7. Roodhart, J. M., Daenen, L. G., Stigter, E. C., Prins, H. J., Gerrits, J., Houthuijzen, J. M., Gerritsen, M. G., Schipper, H. S., Backer, M. J., van Amersfoort, M., Vermaat, J. S., Moerer, P., Ishihara, K., Kalkhoven, E., Beijnen, J. H., Derksen, P. W., Medema, R. H., Martens, A. C., Brenkman, A. B. & Voest, E. E. (2011). Mesenchymal stem cells induce resistance to chemotherapy through the release of platinum-induced fatty acids. Cancer Cell 20, 370-83.

8. Cavill, R., Kamburov, A., Ellis, J. K., Athersuch, T. J., Blagrove, M. S., Herwig, R., Ebbels, T. M. & Keun, H. C. (2011). Consensus-phenotype integration of transcriptomic and metabolomic data implies a role for metabolism in the chemosensitivity of tumour cells. PLoS Comput Biol 7, e1001113.

9. Wang, D. & Lippard, S. J. (2005). Cellular processing of platinum anticancer drugs. Nat Rev Drug Discov 4, 307-20.

10. Mandic, A., Hansson, J., Linder, S. & Shoshan, M. C. (2003). Cisplatin induces endoplasmic reticulum stress and nucleus-independent apoptotic signaling. J Biol Chem 278, 9100-6.

11. Galluzzi, L., Senovilla, L., Vitale, I., Michels, J., Martins, I., Kepp, O., Castedo, M. & Kroemer, G. (2012). Molecular mechanisms of cisplatin resistance. Oncogene 31, 1869-83.

12. Lord, C. J. & Ashworth, A. (2012). The DNA damage response and cancer therapy. Nature 481, 287-94.

13. Carreras Puigvert, J., von Stechow, L., Siddappa, R., Pines, A., Bahjat, M., Haazen, L. C., Olsen, J. V., Vrieling, H., Meerman, J. H., Mullenders, L. H., van de Water, B. & Danen, E. H. (2013). Systems biology approach identifies the kinase csnk1a1 as a regulator of the DNA damage response in embryonic stem cells

Sci. Signal 6, ra5.

14. Pines, A., Kelstrup, C. D., Vrouwe, M. G., Puigvert, J. C., Typas, D., Misovic, B., de Groot, A., von Stechow, L., van de Water, B., Danen, E. H., Vrieling, H., Mullenders, L. H. & Olsen, J. V. (2011). Global phosphoproteome profiling reveals unanticipated networks responsive to cisplatin treatment of embryonic stem cells. Mol Cell Biol 31, 4964-77.

15. Tichy, E. D. (2011). Mechanisms

maintaining genomic integrity in embryonic stem cells and induced pluripotent stem cells. Exp Biol Med (Maywood) 236, 987-96.

16. Ben-David, U. & Benvenisty, N. (2011). The tumorigenicity of human embryonic and induced pluripotent stem cells. Nat Rev Cancer 11, 268-77.

17. Ruiz-Aracama, A., Peijnenburg, A., Kleinjans, J., Jennen, D., van Delft, J., Hellfrisch, C. & Lommen, A. (2011). An untargeted multi-technique metabolomics approach to studying intracellular metabolites of HepG2 cells exposed to 2,3,7,8-tetrachlorodibenzo-p-dioxin. BMC Genomics 12, 251.

18. De Vos, R. C., Moco, S., Lommen, A., Keurentjes, J. J., Bino, R. J. & Hall, R. D. (2007). Untargeted large-scale plant metabolomics using liquid chromatography coupled to mass spectrometry. Nat Protoc 2, 778-91.

19. Lommen, A., Gerssen, A., Oosterink, J. E., Kools, H. J., Ruiz-Aracama, A., Peters, R. J. & Mol, H. G. (2011). Ultra-fast searching assists in evaluating sub-ppm mass accuracy enhancement in U-HPLC/Orbitrap MS data. Metabolomics 7, 15-24.

20. Lommen, A. (2009). MetAlign: interface-driven, versatile metabolomics tool for hyphenated full-scan mass spectrometry data preprocessing. Anal Chem 81, 3079-86.

21. Gao, J., Tarcea, V. G., Karnovsky, A., Mirel, B. R., Weymouth, T. E., Beecher, C. W., Cavalcoli, J. D., Athey, B. D., Omenn, G. S., Burant, C. F. & Jagadish, H. V. (2010). Metscape: a Cytoscape plug-in for visualizing and interpreting metabolomic data in the context of human metabolic networks. Bioinformatics 26, 971-3.

22. Karnovsky, A., Weymouth, T., Hull, T., Tarcea, V. G., Scardoni, G., Laudanna, C., Sartor, M. A., Stringer, K. A., Jagadish, H. V., Burant, C., Athey, B. & Omenn, G. S. (2012). Metscape 2 bioinformatics tool for the analysis and visualization of metabolomics and gene expression data. Bioinformatics 28, 373-80.

23. Pederzolli, C. D., Rockenbach, F. J., Zanin, F. R., Henn, N. T., Romagna, E. C., Sgaravatti, A. M., Wyse, A. T., Wannmacher, C. M., Wajner, M., de Mattos Dutra, A. & Dutra-Filho, C. S. (2009). Intracerebroventricular administration of N-acetylaspartic acid impairs antioxidant defenses and promotes protein oxidation in cerebral cortex of rats. Metab Brain Dis 24, 283-98.

24. Lu, S. C. & Mato, J. M. (2008). S-Adenosylmethionine in cell growth, apoptosis and liver cancer. J Gastroenterol Hepatol 23 Suppl 1, S73-7.

25. Tan, X. L., Moyer, A. M., Fridley, B. L., Schaid, D. J., Niu, N., Batzler, A. J., Jenkins, G. D., Abo, R. P., Li, L., Cunningham, J. M., Sun, Z., Yang, P. & Wang, L. (2011). Genetic variation predicting cisplatin cytotoxicity associated with overall survival in lung cancer patients receiving platinum-based chemotherapy. Clin Cancer Res 17, 5801-11.

26. Morris, S. M., Jr. (2004). Enzymes of arginine metabolism. J Nutr 134, 2743S-2747S; discussion 2765S-2767S.

27. Phang, J. M., Pandhare, J. & Liu, Y. (2008). The metabolism of proline as microenvironmental stress substrate. J Nutr 138, 2008S-2015S.

28. Liu, Y., Borchert, G. L., Surazynski, A. & Phang, J. M. (2008). Proline oxidase, a p53-induced gene, targets COX-2/PGE2 signaling to induce apoptosis and inhibit tumor growth in colorectal cancers. Oncogene 27, 6729-37.

29. Yoon, K. A., Nakamura, Y. & Arakawa, H. (2004). Identification of ALDH4 as a p53-inducible gene and its protective role in cellular stresses. J Hum Genet 49, 134-40.

30. Hubscher, U., Maga, G. & Spadari, S. (2002). Eukaryotic DNA polymerases. Annu Rev Biochem 71, 133-63.

31. Bourdon, A., Minai, L., Serre, V., Jais, J. P., Sarzi, E., Aubert, S., Chretien, D., de Lonlay, P., Paquis-Flucklinger, V., Arakawa, H., Nakamura, Y., Munnich, A.

& Rotig, A. (2007). Mutation of RRM2B, encoding p53-controlled ribonucleotide reductase (p53R2), causes severe mitochondrial DNA depletion. Nat Genet 39, 776-80.

32. Jackson, S. P. & Bartek, J. (2009). The DNA-damage response in human biology and disease. Nature 461, 1071-8.

33. Jones, D. L. & Rando, T. A. (2011). Emerging models and paradigms for stem cell ageing. Nat Cell Biol 13, 506-12.

34. Niehrs, C. (2009). Active DNA demethylation and DNA repair. Differentiation 77, 1-11.

35. Motorin, Y. & Helm, M. (2011). RNA nucleotide methylation. Wiley Interdiscip Rev RNA 2, 611-31.

36. Gehrke, C. W., Kuo, K. C., Waalkes, T. P. & Borek, E. (1979). Patterns of urinary excretion of modified nucleosides. Cancer Res 39, 1150-3.

37. Hsu, W. Y., Chen, W. T., Lin, W. D., Tsai, F. J., Tsai, Y., Lin, C. T., Lo, W. Y., Jeng, L. B. & Lai, C. C. (2009). Analysis of urinary nucleosides as potential tumor markers in human colorectal cancer by high performance liquid chromatography/ electrospray ionization tandem mass spectrometry. Clin Chim Acta 402, 31-7.

38. Seidel, A., Brunner, S., Seidel, P., Fritz, G. I. & Herbarth, O. (2006). Modified nucleosides: an accurate tumour marker for clinical diagnosis of cancer, early detection and therapy control. Br J Cancer 94, 1726-33.

39. Jansen, B. A., Brouwer, J. & Reedijk, J. (2002). Glutathione induces cellular resistance against cationic dinuclear platinum anticancer drugs. J Inorg Biochem 89, 197-202.

40. Chen, H. H. & Kuo, M. T. (2010). Role of glutathione in the regulation of Cisplatin resistance in cancer chemotherapy. Met Based Drugs 2010.

41. Wang & Guo, Z. (2007). The role of sulfur in platinum anticancer chemotherapy. Anticancer Agents Med Chem 7, 19-34.

42. Yan, X. D., Pan, L. Y., Yuan, Y., Lang, J. H. & Mao, N. (2007). Identification of platinum-resistance associated proteins through proteomic analysis of human ovarian cancer cells and their platinum-resistant sublines. J Proteome Res 6, 772-80.

43. Whitbread, A. K., Masoumi, A., Tetlow, N., Schmuck, E., Coggan, M. & Board, P. G. (2005). Characterization of the omega class of glutathione transferases. Methods Enzymol 401, 78-99.

44. Christensen, K. E. & Mackenzie, R. E. (2008). Mitochondrial methylenetetrahydrofolate dehydrogenase, methenyltetrahydrofolate cyclohydrolase, and formyltetrahydrofolate synthetases. Vitam Horm 79, 393-410.

45. Assaraf, Y. G. (2007). Molecular basis of antifolate resistance. Cancer Metastasis Rev 26, 153-81.

46. Hector, S., Porter, C. W., Kramer, D. L., Clark, K., Prey, J., Kisiel, N., Diegelman, P., Chen, Y. & Pendyala, L. (2004). Polyamine catabolism in platinum drug action: Interactions between oxaliplatin and the polyamine analogue N1,N11-diethylnorspermine at the level of spermidine/spermine N1-acetyltransferase. Mol Cancer Ther 3, 813-22.

47. Cervelli, M., Amendola, R., Polticelli, F. & Mariottini, P. (2012). Spermine oxidase: ten years after. Amino Acids 42, 441-50.

48. Loffler, M., Fairbanks, L. D., Zameitat, E., Marinaki, A. M. & Simmonds, H. A. (2005). Pyrimidine pathways in health and disease. Trends Mol Med 11, 430-7.

49. Welin, M. & Nordlund, P. (2010). Understanding specificity in metabolic pathways--structural biology of human nucleotide metabolism. Biochem Biophys Res Commun 396, 157-63.

50. Krishnan, N., Dickman, M. B. & Becker, D. F. (2008). Proline modulates the intracellular redox environment and protects mammalian cells against oxidative stress. Free Radic Biol Med 44, 671-81.

SUPPLEMENTARY MATERIALS

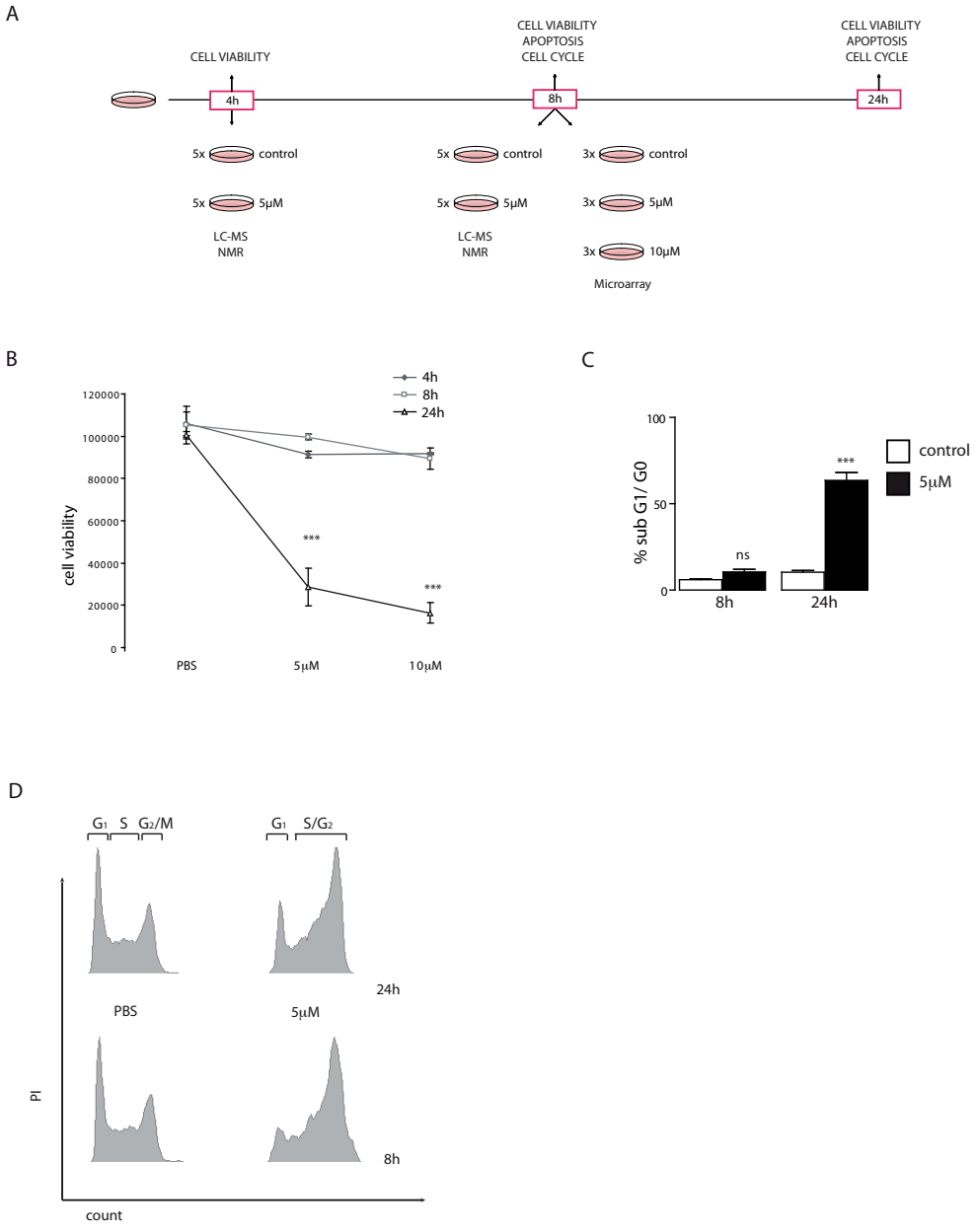

Figure S1. Cisplatin does not lead to cell death at 4 h and 8 h of treatment, but causes cell cycle arrest. (A) Schematic representation of the experiments. (B) Cell viability measured by ATPlite in ES cells after treatment with 5 μM and 10 μM cisplatin at 4 h, 8 h and 24 h of treatment. (C) Apoptosis measured by FACS analysis after 8 h and 24 h of treatment with 5 μM cisplatin. (D) Cell cycle profile after 8 h and 24 h treatment with PBS or 5 μM cisplatin.

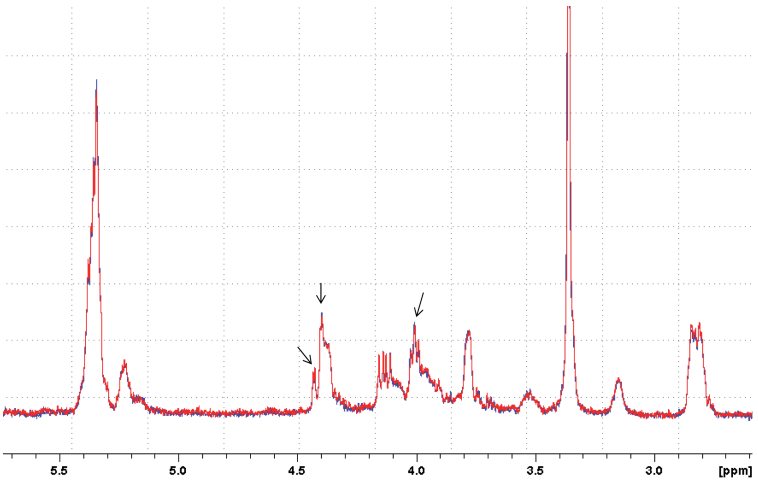

Figure S2. Expanded region between 5.5 and 2.5 ppm of a 1HNMR spectrum of the apolar extract of HM1 ESC after 8 h of exposure to cisplatin (blue) and to vehicle (red). Arrows indicate characteristic phospholipid signals.

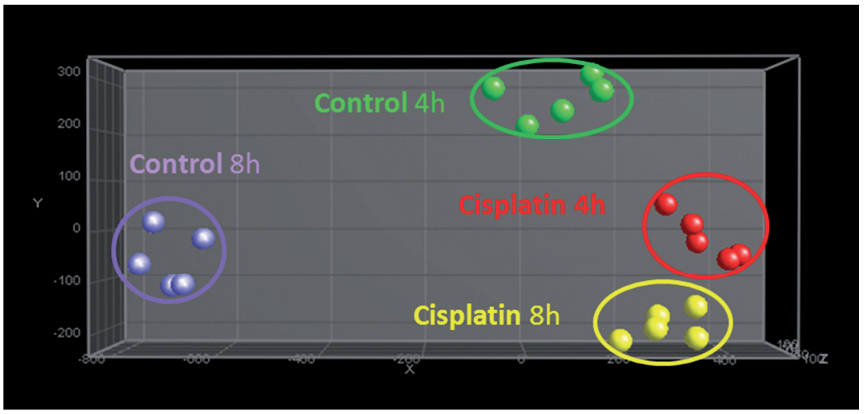

Figure S3. Regulation of metabolites in cisplatin and control group at different timepoints. PCA plots of aligned U-HPLC-Orbitrap-MS data after pre-selection using 2Log transformation and an ANOVA ($p < 0.01$), Samples grouped on biological replicates.

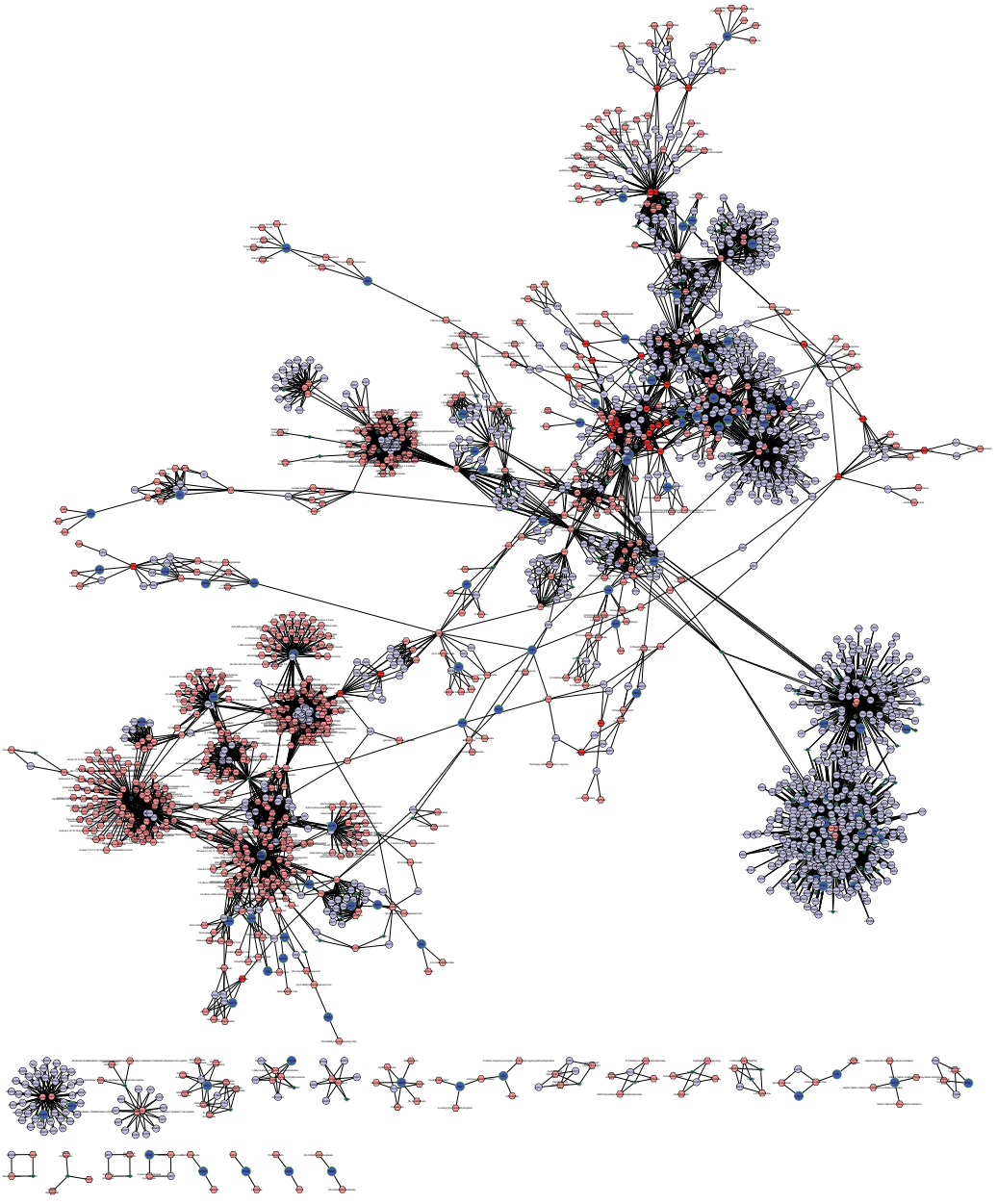

Figure S4. Metscape "gene-compound metabolic network". Highlighted in yellow are compounds and genes showing a significant regulation after 4 h cisplatin treatment. Metabolic enzymes were retrieved from this network (Fig 2A, TableS 2).

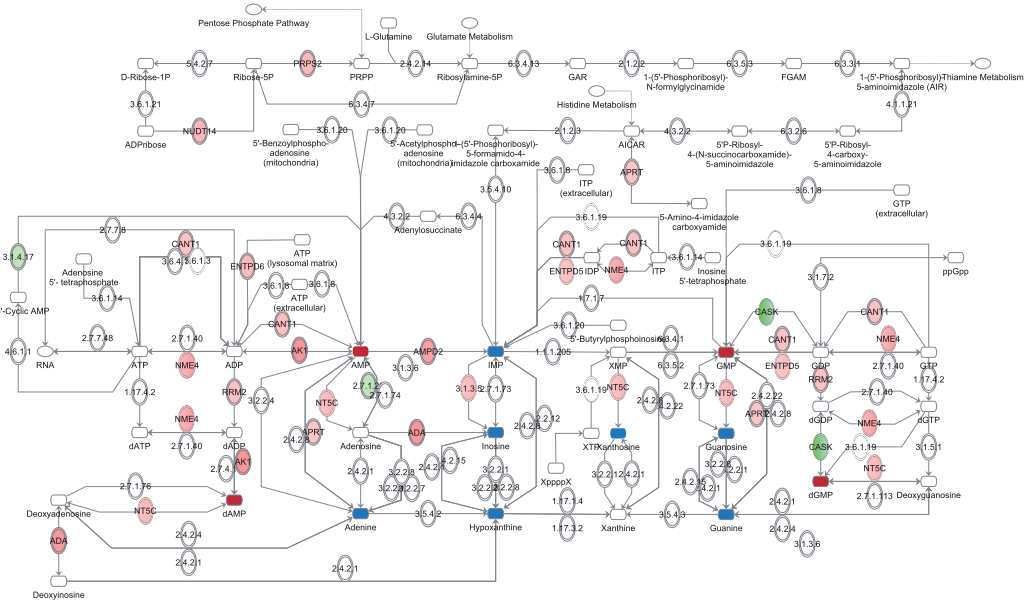

Purine metabolism

Figure S5. Purine metabolism. Upregulated enzymes in green, downregulated enzymes in red. Upregulated metabolites in dark red, downregulated metabolites in blue.

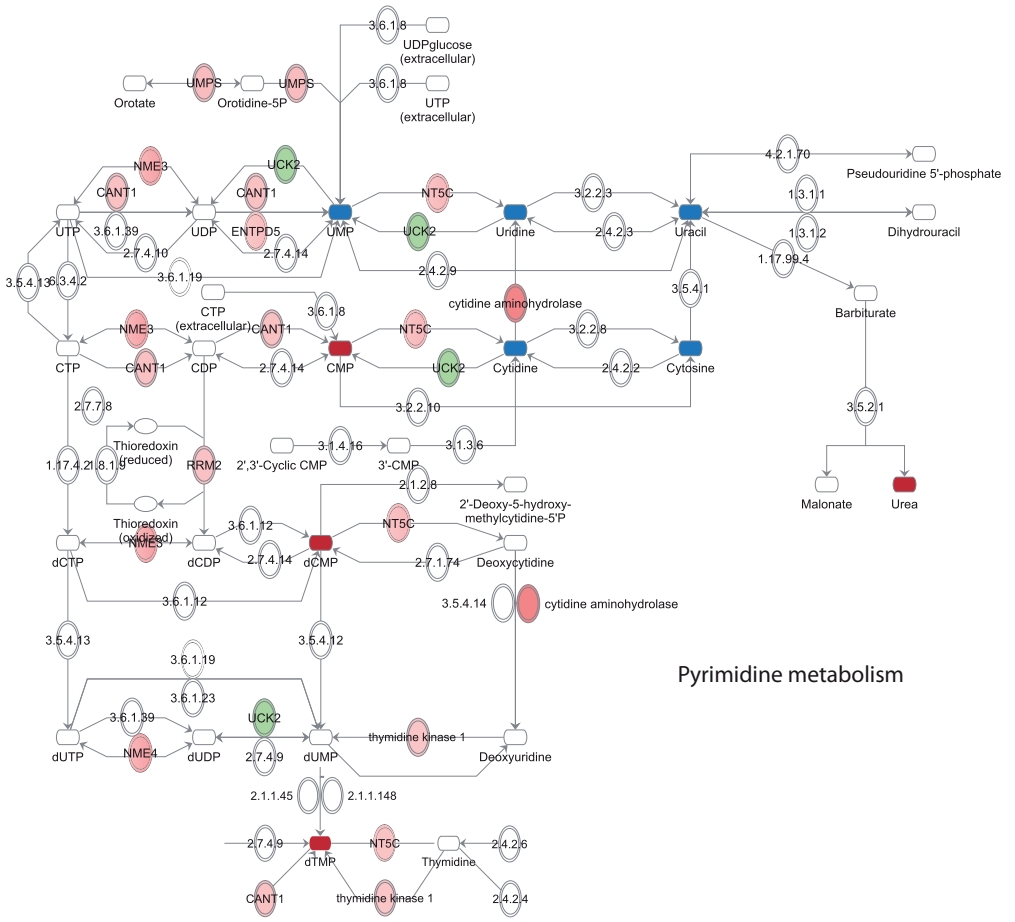

Figure S6. Pyrimidine metabolism. Upregulated enzymes in green, downregulated enzymes in red. Upregulated metabolites in dark red, downregulated metabolites in blue.

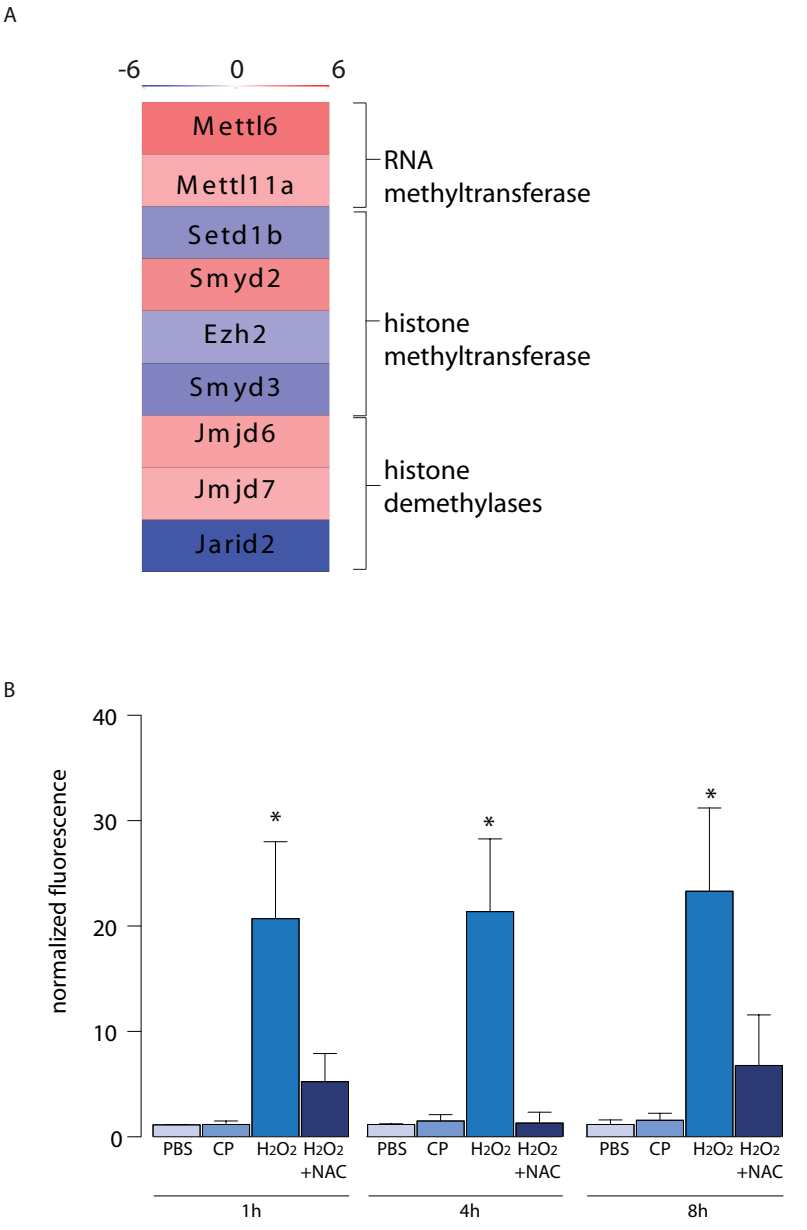

Figure S7. (A) Regulation of (de)methylases. Heatmap showing regulation of methyltransferases and demethylases after cisplatin treatment. **(B) ROS formation is caused by hydrogen peroxide but not cisplatin treatment.** Bar graph shows normalized fluorescence indicating intracellular ROS levels measured using 40 µM DCF-DA probe. Cells were preincubated with DCF-DA for 1 h and exposed to 5 µM cisplatin or 250 µM H2O2 in the presence or absence of 10 mM of the ROS scavenger NAC for the indicated times. Bars represent average and SEM of at least 3 independent experiments.

								Treatment and signal intensity			
Metabolite	Experimental adduct MW (Da)	Theoretical adduct MW (Da)	Delta	Ppm	Chemical Formula	MS/MS fragments (M+1)	Control 4h	Control 8h	Cis-Pt 4h	Cis-Pt 8h
3-Methylcytidine	258.10837	258.10845	0.00008	0.30607	C10H15N3O5	126.0652	43659	69975.6	27447.8	32724.4
4-Methylcytidine	258.10837	258.10845	0.00008	0.30607	C10H15N3O5	126.0649	66868	4408818.6	43317.2	60254.4
Adenine	136.061798	136.06177	-0.00003	-0.20579	C5H5N5		98387.2	155167	69237.4	126605.2
AMP	348.07037	348.0704	0.00003	0.086189461	C10H14N5O7P		15901506.4	19642998	24374196.8	22618056
Camitine	162.11241	162.11247	0.00006	0.35778	C7H15NO3		74118.2	137013.2	108002.2	125298.2
CMP	324.05914	324.05913	-0.00002	-0.04937	C9H14N3O8P	112.0501	1955741	1972786	2383394.2	2103885.8
Cytidine	244.09279	244.0928	0.00001	0.03277	C9H13N3O5	112.0501	13526183.4	11633406.8	10484320.6	9615623.6
Cytosine	112.05041	112.05054	0.00013	1.16912	C4H5N3O		228957	186960.2	169188.4	158458
dCMP	308.06412	308.06421	0.00009	0.30838	C9H14N3O7P		1143933.4	107660.8	151089	142592.4
dTMP	323.06384	323.06388	0.00003	0.10834	C10H15N2O8P		66191.4	85536.6	108300.6	119938.2
Glutathione_ox	307.083221	307.083257 (2M+1)	0.00004	0.11723	C20H32N6O12S2		2017249.6	2045477	2567759.8	1979258.2
Glutathione_red	308.091034	308.09108	0.00005	0.1558	C10H17N3O6S		29952953.2	28493909.6	42463695.2	33234441.6
GMP	364.06537	364.06528	-0.00009	-0.2582	C10H14N5O8P	152.0563 -> 135.0296, 110.0343	2096198.4	2372360.2	2605548.6	2739346
Guanine	152.05673	152.05669	-0.00005	-0.30252	C5H5N5O		2820315	2325012.6	2184768	1992020.2
Guanosine	284.09882	284.09895	0.00013	0.45407	C10H13N5O5	152.0562 -> 135.0297, 110.0349	5045863	4541230.8	3986165.6	4393332
Homocysteine	136.04274	136.04268	-0.00007	-0.47779	C4H9NO2S		30950	40046	42819.8	36480.8
Homoserine	120.06542	120.06552	0.0001	0.80789	C4H9NO3		1919764.2	1805556.6	2625698.4	1920786
Hypoxanthine	137.04588	137.04579	-0.0001	-0.7005	C5H4N4O		13456075.2	14786181.2	12442760	11983405.8
IMP	349.05426	349.05438	0.00012	0.33233	C10H13N4O8P		121369	414232.6	131602.8	139221.6
Methionine	150.058411	150.05833	-0.00009	-0.57311	C5H11NO2S		7706583.8	10818675.2	10570783.8	9986466.2
Methylthioadenosine	298.096832	298.09684	0.00001	0.02684	C11H15N5O3S		450473.2	756566.8	537241.4	803968
N-Acetylaspartate	176.055313	176.05535	0.00003	0.1988	C6H9NO5		147380.8	123233.2	190853.4	141058.6
N-Acetylaspartylglutamate	305.097839	305.09794	0.0001	0.33432	C11H16N2O8		161337	162741.6	188373	155566.4
N-Acetylputrescine	131.117676	131.11789	0.00021	1.62449	C6H14N2O		131137.6	198542.2	185212.2	215285.4
Pantothenic acid	220.11792	220.11795	0.00003	0.13175	C9H17NO5		1266479.2	2226354.2	1698029.4	2057904.6
Proline	116.070549	116.07061	0.00006	0.48246	C5H9NO2		172001366	101223388	24880710	16813324.4
Putrescine	119.081436	119.0815	0.00007	0.57104	C4H10N2O2		9654137	19608510.4	14285301.6	21220009.2
S-Adenosylhomocysteine	385.128937	385.12886	-0.00007	-0.18955	C14H20N6O5S		328136	572516.4	454726.8	479502
S-Adenosylmethionine	399.144714	399.14451	-0.0002	-0.51109	C15H22N6O5S		82934.4	116946.6	133855.8	146548.6
Spermine	203.222992	203.22302	0.00003	0.15254	C10H26N4	97.0279	785843.6	1470363.8	1029575	1439971.4
UMP	325.043152	325.04314	-0.00001	-0.02769	C9H13N2O9P		952727	1082367.4	808426.2	920139.4
Uracil	113.034431	113.03455	0.00012	1.07932	C4H4N2O2		5043693.2	3142124	2276664	187734
Urea	121.07164	121.072002 (2M+1)	0.00036	2.98996	CH4N2O	113.0341	936447.6	815119.2	1292005.6	891853.6
Uridine	245.076797	245.07681	0.00001	0.06121	C9H12N2O6		673773	5284746	449850.2	509529.8
Xanthosine	285.082886	285.08296	0.00007	0.25957	C10H12N4O6		27491.2	43998.2	16772.4	17957.6

Table S1. Identified metabolites. Identification of masses found to be significantly different ($p<0.01$) between control and cisplatin-treated samples.

gene symbol	gene name	fold change
MLL3	myeloid/lymphoid or mixed-lineage leukemia 3	-7.69
EXT1	exostoses (multiple) 1	-6.67
FUT8	fucosyltransferase 8 (alpha (1,6) fucosyltransferase)	-5.26
Ppp3ca	protein phosphatase 3, catalytic subunit, alpha isoform	-4.76
DSE	dermatan sulfate epimerase	-4.76
PIK3CB	phosphatidylinositol-4,5-bisphosphate 3-kinase, catalytic subunit beta	-3.70
ATP2B1	ATPase, Ca++ transporting, plasma membrane 1	-3.70
PPAP2B	phosphatidic acid phosphatase type 2B	-3.57
PPAP2B	phosphatidic acid phosphatase type 2B	-3.57
ENPP3	ectonucleotide pyrophosphatase/phosphodiesterase 3	-3.45
FARS2	phenylalanyl-tRNA synthetase 2, mitochondrial	-3.23
PLCH1	phospholipase C, eta 1	-3.13
UCK2	uridine-cytidine kinase 2	-3.12
PIP4K2A	phosphatidylinositol-5-phosphate 4-kinase, type II, alpha	-3.03
OXCT1	3-oxoacid CoA transferase 1	-3.03
POLA1	polymerase (DNA directed), alpha 1, catalytic subunit	-2.94
ST6GAL1	ST6 beta-galactosamide alpha-2,6-sialyltranferase 1	-2.86
SMYD3	SET and MYND domain containing 3	-2.78
ATP11C	ATPase, class VI, type 11C	-2.78
PTEN	phosphatase and tensin homolog	-2.78
GALNT1	UDP-N-acetyl-alpha-D-galactosamine:polypeptide N-acetylgalactosaminyltransferase 1 (GalNAc-T1)	-2.70
POLR3A	polymerase (RNA) III (DNA directed) polypeptide A, 155kDa	-2.70
ITPK1	inositol-tetrakisphosphate 1-kinase	-2.63
GPD2	glycerol-3-phosphate dehydrogenase 2 (mitochondrial)	-2.63
GALNT7	UDP-N-acetyl-alpha-D-galactosamine:polypeptide N-acetylgalactosaminyltransferase 7 (GalNAc-T7)	-2.63
PCYT1B	phosphate cytidylyltransferase 1, choline, beta	-2.44
POLR3B	polymerase (RNA) III (DNA directed) polypeptide B	-2.44
POLR3B	polymerase (RNA) III (DNA directed) polypeptide B	-2.44
ELOVL6	ELOVL fatty acid elongase 6	-2.38
MBOAT2	membrane bound O-acyltransferase domain containing 2	-2.38
PFKP	phosphofructokinase, platelet	-2.33
WHSC1L1	Wolf-Hirschhorn syndrome candidate 1-like 1	-2.33
IP6K1	inositol hexakisphosphate kinase 1	-2.33
Lclat1	lysocardiolipin acyltransferase 1	-2.17
TPK1	thiamin pyrophosphokinase 1	-2.17
PCMT1	protein-L-isoaspartate (D-aspartate) O-methyltransferase	-2.08
B4GALT5	UDP-Gal:betaGlcNAc beta 1,4- galactosyltransferase, polypeptide 5	-2.08
PCCA	propionyl Coenzyme A carboxylase, alpha polypeptide	-2.08
ADK	adenosine kinase	-2.08
PDE3B	phosphodiesterase 3B, cGMP-inhibited	-2.08
PLCB4	phospholipase C, beta 4	-2.04
SEPHS1	selenophosphate synthetase 1	-2.04
CDS2	CDP-diacylglycerol synthase (phosphatidate cytidylyltransferase) 2	-2.00
ATP10A	ATPase, class V, type 10A	-1.85
GRK5	G protein-coupled receptor kinase 5	-1.79
FARSB	phenylalanyl-tRNA synthetase, beta subunit	-1.75

gene symbol	gene name	fold change
BDH2	3-hydroxybutyrate dehydrogenase, type 2	-1.72
PLCG2	phospholipase C, gamma 2 (phosphatidylinositol-specific)	-1.69
SLC27A2	solute carrier family 27 (fatty acid transporter), member 2	-1.69
PAFAH1B1	platelet-activating factor acetylhydrolase, isoform Ib, subunit 1 (45kDa)	-1.67
PLCB1	phospholipase C, beta 1 (phosphoinositide-specific)	-1.67
STT3B	STT3, subunit of the oligosaccharyltransferase complex, homolog B (S. cerevisiae)	-1.64
MTHFD1L	methylenetetrahydrofolate dehydrogenase (NADP+ dependent) 1-like	-1.64
HSD17B12	hydroxysteroid (17-beta) dehydrogenase 12	-1.59
DGKH	diacylglycerol kinase, eta	-1.52
PTPN13	protein tyrosine phosphatase, non-receptor type 13 (APO-1/CD95 (Fas)-associated phosphatase)	-1.52
POLR1A	polymerase (RNA) I polypeptide A, 194kDa	-1.49
SMS	spermine synthase	-1.41
ASNS	asparagine synthetase	-1.39
GBA	glucosidase, beta; acid (includes glucosylceramidase)	-1.33
POLB	polymerase (DNA directed), beta	1.31
FECH	ferrochelatase (protoporphyria)	1.39
FUK	fucokinase	1.40
ACAA2	acetyl-Coenzyme A acyltransferase 2	1.41
PRODH	proline dehydrogenase (oxidase) 1	1.42
NPR2	natriuretic peptide receptor B/guanylate cyclase B (atrionatriuretic peptide receptor B)	1.42
ENTPD5	ectonucleoside triphosphate diphosphohydrolase 5	1.43
POLR3K	polymerase (RNA) III (DNA directed) polypeptide K, 12.3 kDa	1.44
PYCR2	pyrroline-5-carboxylate reductase family, member 2	1.45
POLR2G	polymerase (RNA) II (DNA directed) polypeptide G	1.45
PPM1F	protein phosphatase, Mg2+/Mn2+ dependent, 1F	1.46
SGPP1	sphingosine-1-phosphate phosphatase 1	1.47
GRHPR	glyoxylate reductase/hydroxypyruvate reductase	1.47
CYP27A1	cytochrome P450, family 27, subfamily A, polypeptide 1	1.49
TK1	thymidine kinase 1, soluble	1.49
AGPAT5	1-acylglycerol-3-phosphate O-acyltransferase 5 (lysophosphatidic acid acyltransferase, epsilon)	1.50
AGPAT5	1-acylglycerol-3-phosphate O-acyltransferase 5 (lysophosphatidic acid acyltransferase, epsilon)	1.50
NANS	N-acetylneuraminic acid synthase	1.50
GAA	glucosidase, alpha; acid	1.51
SMPD4	sphingomyelin phosphodiesterase 4, neutral membrane (neutral sphingomyelinase-3)	1.52
APRT	adenine phosphoribosyltransferase	1.53
RRM2	ribonucleotide reductase M2	1.53
MCAT	malonyl CoA:ACP acyltransferase (mitochondrial)	1.54
ECHDC2	enoyl Coenzyme A hydratase domain containing 2	1.55
FPGS	folylpolyglutamate synthase	1.55
MLYCD	malonyl-CoA decarboxylase	1.58
PGLS	6-phosphogluconolactonase	1.58
MECR	mitochondrial trans-2-enoyl-CoA reductase	1.58
DPM2	dolichyl-phosphate mannosyltransferase polypeptide 2, regulatory subunit	1.60
ALDH4A1	aldehyde dehydrogenase 4 family, member A1	1.61
HMGCL	3-hydroxymethyl-3-methylglutaryl-Coenzyme A lyase	1.63

gene symbol	gene name	fold change
CANT1	calcium activated nucleotidase 1	1.65
Prkcd	protein kinase C, delta	1.65
ACAT2	acetyl-Coenzyme A acetyltransferase 2	1.66
ACADS	acyl-Coenzyme A dehydrogenase, C-2 to C-3 short chain	1.66
PMM1	phosphomannomutase 1	1.69
GPT	glutamic-pyruvate transaminase (alanine aminotransferase)	1.69
DGKA	diacylglycerol kinase, alpha 80kDa	1.70
CBR3	carbonyl reductase 3	1.70
GLS	glutaminase	1.70
PARS2	prolyl-tRNA synthetase 2, mitochondrial (putative)	1.71
MDP1	magnesium-dependent phosphatase 1	1.73
POLE3	polymerase (DNA directed), epsilon 3 (p17 subunit)	1.73
PLOD3	procollagen-lysine, 2-oxoglutarate 5-dioxygenase 3	1.75
POLL	polymerase (DNA directed), lambda	1.76
NDUFB2	NADH dehydrogenase (ubiquinone) 1 beta subcomplex, 2, 8kDa	1.77
DGKZ	diacylglycerol kinase, zeta 104kDa	1.78
DHFR	dihydrofolate reductase	1.78
UMPS	uridine monophosphate synthetase	1.78
PAFAH2	platelet-activating factor acetylhydrolase 2, 40kDa	1.80
FAH	fumarylacetoacetate hydrolase (fumarylacetoacetase)	1.80
ENTPD6	ectonucleoside triphosphate diphosphohydrolase 6 (putative function)	1.80
POLR2D	polymerase (RNA) II (DNA directed) polypeptide D	1.85
TPMT	thiopurine S-methyltransferase	1.87
MCEE	methylmalonyl CoA epimerase	1.89
PRPS2	phosphoribosyl pyrophosphate synthetase 2	1.89
AMPD2	adenosine monophosphate deaminase 2 (isoform L)	1.89
NME4	non-metastatic cells 4, protein expressed in	1.90
NT5C	5', 3'-nucleotidase, cytosolic	1.93
GATM	glycine amidinotransferase (L-arginine:glycine amidinotransferase)	1.98
GSTO1	glutathione S-transferase omega 1	2.04
PMVK	phosphomevalonate kinase	2.05
IVD	isovaleryl Coenzyme A dehydrogenase	2.08
CERCAM	cerebral endothelial cell adhesion molecule	2.11
FBP2	fructose-1,6-bisphosphatase 2	2.14
LPIN1	lipin 1	2.22
CBS	cystathionine-beta-synthase	2.22
SPR	sepiapterin reductase (7,8-dihydrobiopterin:NADP+ oxidoreductase)	2.39
DECR2	2,4-dienoyl CoA reductase 2, peroxisomal	2.39
ABHD5	abhydrolase domain containing 5	2.40
AACS	acetoacetyl-CoA synthetase	2.41
PTS	6-pyruvoyltetrahydropterin synthase	2.49
VKORC1	vitamin K epoxide reductase complex, subunit 1	2.66
NME3	non-metastatic cells 3, protein expressed in	2.72
SORD	sorbitol dehydrogenase	2.76
GNE	glucosamine (UDP-N-acetyl)-2-epimerase/N-acetylmannosamine kinase	2.82
ADA	adenosine deaminase	2.99
CPT1C	carnitine palmitoyltransferase 1C	3.01
AK1	adenylate kinase 1	3.08

gene symbol	gene name	fold change
SMOX	spermine oxidase	3.27
ELOVL2	ELOVL fatty acid elongase 2	3.38
ADC	arginine decarboxylase	3.75
Apobec1	apolipoprotein B mRNA editing enzyme, catalytic polypeptide 1	3.76
EPHX1	epoxide hydrolase 1, microsomal (xenobiotic)	4.74

Table S2. Significantly regulated metabolic enzymes. List of metabolic enzymes identified by Metscape and Ingenuity pathway analysis from 2269 genes that are differentially regulated by cisplatin.

Orbitrap Mass Spectrometer settings

Heated electrospray interface (HESI): operating in positive mode (ESI^+).

Data acquisition: between m/z 100 and m/z 1000

Resolving power: 50.000 (FWHM)

Scan time: 0.5 s

Spray voltage: 2800 V

Capillary voltage: 47.5 V

Capillary temperature: 250 ˚C

Sheath gas flow: 19 arbitrary units

Auxiliary gas flow: 7 arbitrary units

Instrument calibration: externally, prior to sequence by infusion of calibration solution (m/z 138 to m/z 1822) containing caffeine, MFRA (Met-Arg-Phe-Ala), ultramark 1621, acetic acid in acetonitrile/methanol/water (2:1:1, v/v) (Sigma-Aldrich).

Material S1. MS Instrument Settings.